

Analysis of p - y Curves from Lateral Load Test of Large Diameter Drilled Shaft in Stiff Clay

Kerop D. Janoyan, Jonathan P. Stewart, and John W. Wallace
University of California, Los Angeles, CA.

Abstract

Analysis and design procedures for cast-in-drilled-hole (CIDH) bridge foundations commonly involve the use of a beam on a nonlinear Winkler foundation (p - y) analysis. The p - y curves used in practice are derived from lateral load testing of relatively small diameter driven piles (diameter, $d < 24$ in or 610 mm). These curves were typically inferred from limited field measurements of pile curvature and with the assumption of a linear pile. In this paper, we develop p - y curves from the measured lateral response of a $d = 6$ ft (1.8 m) CIDH shaft/column in stiff clay that was subjected to a wide range of lateral cyclic displacement amplitudes. Multiple instrumentation sources provide redundant section curvature measurements, which enable the variability in the nonlinear soil reaction (i.e., p -values) to be quantified. Moreover, we find that accounting for the nonlinear behavior of the reinforced concrete section significantly affects p -values, an effect not widely considered in previous studies.

Introduction

Cast-in-drilled-hole (CIDH) shaft/columns have been widely used for the support of highway bridges in California and elsewhere due to their cost-effective and space-saving features. The behavior of the shaft foundations under earthquake loading is an important consideration in design. Analysis and design procedures for evaluating shaft behavior under lateral loading commonly involve the use of a beam on a nonlinear Winkler foundation (p - y) analysis. The p - y curves used in practice (e.g., API, 1993) are based, for the most part, on the results of full-scale experiments on relatively small diameter piles as summarized below:

- Soft clays w/ free water: 12.75 inch (324 mm) diameter steel-pipe piles (Matlock, 1970)
- Stiff clays w/ free water: 24 inch (610 mm) diameter steel-pipe piles (Reese et al., 1975)
- Stiff clays w/o free water: 36 inch (915 mm) diameter reinforced concrete drilled shaft (Reese and Welch, 1975)
- Sands: 24 inch (610 mm) diameter steel-pipe piles (Cox, et al., 1974)

Note that many of these tests were conducted on steel-pipe piles, which are relatively easy to instrument with electrical-resistance strain gauges (for measurement of section curvature). Ground-line deflection and rotation of the piles were typically measured using LVDTs and inclinometers, respectively. As discussed subsequently in the paper, p -values inferred from such tests are highly sensitive to small variations in field curvature measurements. Such variability has not been quantified in most previous tests, and hence the reliability of these “standard” p - y

curves is unknown. Moreover, in large-deflection lateral load tests, measured curvature data reflect nonlinearity in both the soil and pile, yet traditional methods for deriving p -values assume a linear pile, thus lumping all nonlinearity into the p - y curve. For modern analyses in which nonlinearity in both soil and pile can be easily incorporated, there is a need for reliable p - y curves that reflect only the nonlinearity of soil-shaft interaction.

In this research, we have developed techniques to evaluate p -values from field lateral load tests that incorporate variability in curvature measurements and structural nonlinearity in bending. These techniques were developed to enable a rational reduction of data from testing of a full-scale large diameter drilled shaft subjected to cyclic lateral loading. In the following sections, we describe the testing program, including instrumentation, structural details, and geotechnical site conditions. We then describe the methods by which p - y curves were inferred from the data, and compare experimental p - y curves to results of various existing predictive techniques.

Drilled Shaft Test Setup and Instrumentation

Test Setup

The CIDH shaft-column was designed according to standard Caltrans' Bridge Design Specifications (1995) using the Seismic Design Criteria (1999). The test specimen was 6 ft (1.8 m) in diameter and extended 48 ft (14.6 m) below ground line and 40 ft (12.2 m) above. As shown in Figure 1, steel reinforcement was comprised of 36-#14 longitudinal bars with average yield and ultimate tensile strengths of 71 ksi (490 MPa) and 102 ksi (703 MPa), respectively, and shop-welded #8 hoops at 6 inch (152 mm) spacing with average yield and ultimate tensile strength of 72 ksi (496 MPa) and 107 ksi (738 MPa), respectively. The longitudinal and transverse steel ratios are ~2% and ~0.7%, respectively. Normal-weight ready-mix concrete was used in the test shaft-column, with the target compressive strength of 3.5 ksi (24 MPa); however, the average tested cylinder compressive strength was 6.1 ksi (42 Mpa).

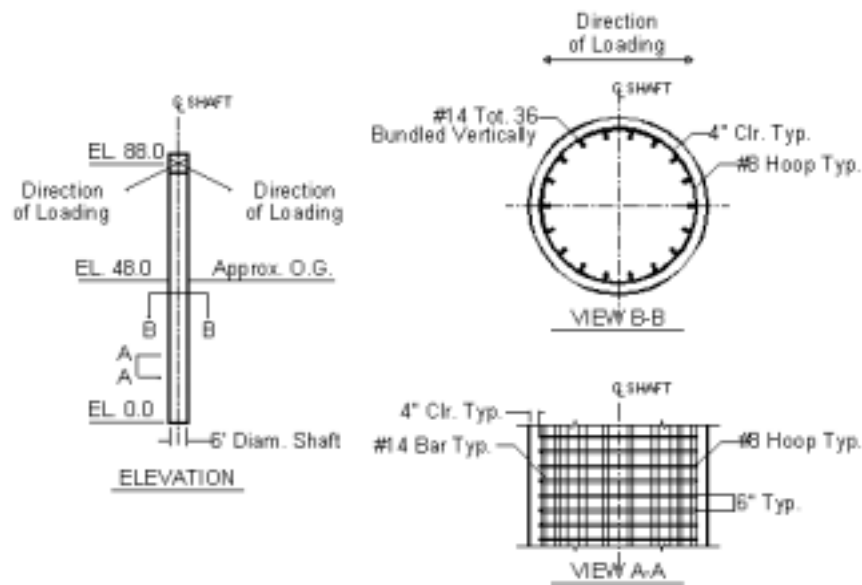


Figure 1: Shaft/column section reinforcement details

Lateral loads were imposed on the column using tension cables reacting against soil anchors. A yoke system installed near the soil anchors imparted tension to the cables. The yoke system consisted of four 100-kip (445 kN) jacks installed between a top beam rigidly connected to screw rods, and a moveable bottom beam to which the cables were connected through a load cell. The jacks have roughly 14 inches (355 mm) of useable stroke, but by resetting the position of the top beam on the screw rods, the yoke system allowed movements of +/- 12 ft (3.6 m) from the original shaft position. A schematic illustration of the loading system is shown in Figure 2.

Testing of the shaft/column was displacement controlled. Cyclic lateral loading was applied across an amplitude range of 2 to 108 inches (50 mm to 2.75 m). Two loading cycles were performed at most displacement levels; however, 12 loading cycles were performed at two displacement amplitudes (6 and 18 inches or 152 and 457 mm) to investigate the effects of cyclic degradation. Cycles at displacement amplitudes > 6 inches (152 mm) included 16 stops to enable measurements of the shape of hysteretic response curves.

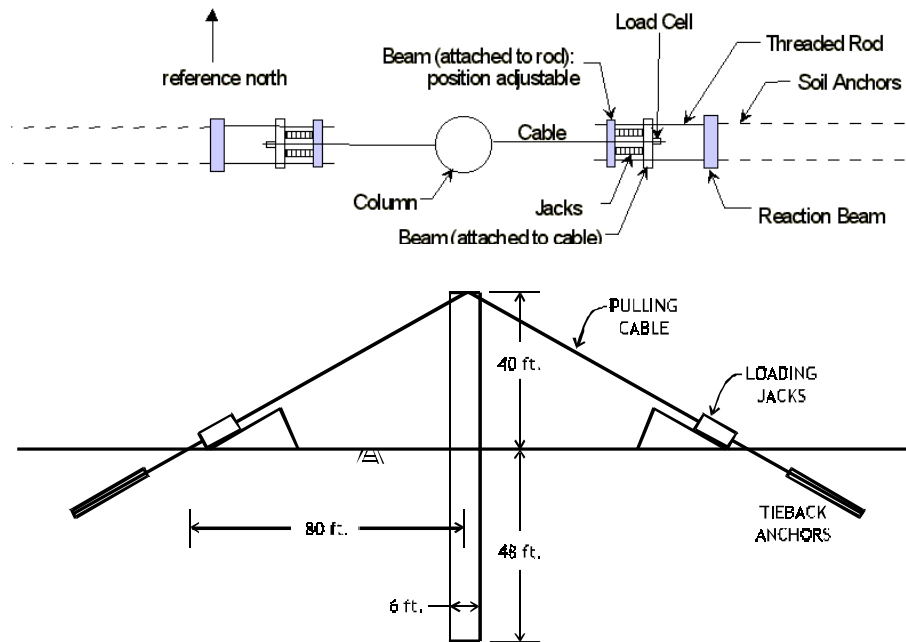


Figure 2: Schematic plan and profile views of loading system

Instrumentation

Extensive instrumentation, totaling over 200 channels of data, was used to monitor the response of the soil/shaft system and the local deformation of the column. Load cells were placed between the pulling cable and the yoke system to measure the force in the pulling cables and thus the horizontal and vertical forces on the top of the column. The deformation of the above-ground column was measured using 12 survey/total stations while the tilt at and below ground level shaft was measured using 11 inclinometers placed down the middle of the shaft.

Shaft and column bending deformations were measured with a redundant system of extensometers, fiber optic sensors, inclinometers and strain gauges. A total of 32 fiber optic sensors were used to measure axial strain in the shaft, each having a 4 ft (1.2 m) gauge length

and a strain range limited to 1% in tension and 0.5% in compression. The fiber optic sensors were placed in pairs close to the extreme fibers of the shaft/column so that curvatures could be inferred from the data. The fiber optic sensors have very high resolution but operate in a limited strain range. Thus, within the anticipated plastic hinge region where large (inelastic) deformations take place, curvature was also measured using 32 extensometers fabricated using potentiometers encased in PVC pipe. These extensometers have a working range of 10% in tension and 4% in compression and a 2 ft (0.6 m) gauge length. One set of extensometers was installed just inside of the reinforcing cage and a second set was installed mid-way between the shaft centroid and reinforcing cage.

Additional instrumentation included 76 electrical resistance strain gauges, 26 soil pressure cells, 10 time-domain-reflectometry cables and 6 gamma test sensor tubes (to measure the quality of the as-placed concrete).

Geotechnical Conditions at Test Site

The test site is located near the intersection of Interstate Highways 105 and 405 in Hawthorne, California. The mapped local geology is Quaternary alluvium. Field in-situ and laboratory testing was performed to characterize the soil conditions at the site. The field testing included seismic cone penetration testing (SCPT), rotary-wash borings with standard penetration testing (SPT), down-hole suspension logging of shear wave velocities, pressuremeter testing (PMT), and test pit excavation mapping. Samples for laboratory testing were retrieved from the borings using thin-walled Pitcher tubes, and were hand-carved from the walls of the test pit. Laboratory testing was performed to evaluate particle size distribution, Atterberg limits, shear strength, and consolidation characteristics.

A simple representation of the soil profile is shown in Figure 3. Major stratigraphic features include:

- 0 to 2-5 feet (0.6-1.5 m): Fill with asphalt and concrete debris.
- 2-5 (0.6-1.5 m) to 18-24 feet (5.5-7.3 m) [Formation 1]: Silty clay layer with a 2 ft (0.6 m) thick silty sand interbed at a depth of approximately 12 ft (3.6 m). CPT testing indicates that in the silty clay, soil behavior type index $I_c \approx 2.6-2.9$ which are typical values for clayey silts and silty clays (Robertson, 1990). Laboratory testing indicates a fines content of approximately 60, $LL = 34$, and $PL = 19$, leading to a soil classification of CL by the Unified Soil Classification System.
- 24 to 28 feet (7.3-8.5 m) [Formation 2]: Medium- to fine-grained silty sand/sandy silt. Values of $I_c \approx 2.1$ were obtained, which are typical of clean to silty sands (Robertson, 1990).
- 20-28 to 48 feet (6.1-8.5 to 14.6 m) [Formation 3]: Silty clay, with $I_c \approx 2.8-3.1$. This layer extends to the base of the shaft, and is underlain by a water-bearing medium sand.

Consolidation testing of the predominant clayey soils was performed according to ASTM D-2435. Overconsolidation ratios (OCR's) in the upper portion of the clay [depth < about 24 ft (7.3 m)] are uncertain because of unknown matric suction in the unsaturated soil. The lower-bound effective stress is the total stress shown in Fig. 3, and based on this stress the upper-bound OCR's are about five. The clays appear to be nearly normally consolidated at depths > 24 ft (7.3 m). Coefficients of consolidation in overconsolidated and normally consolidated increments of

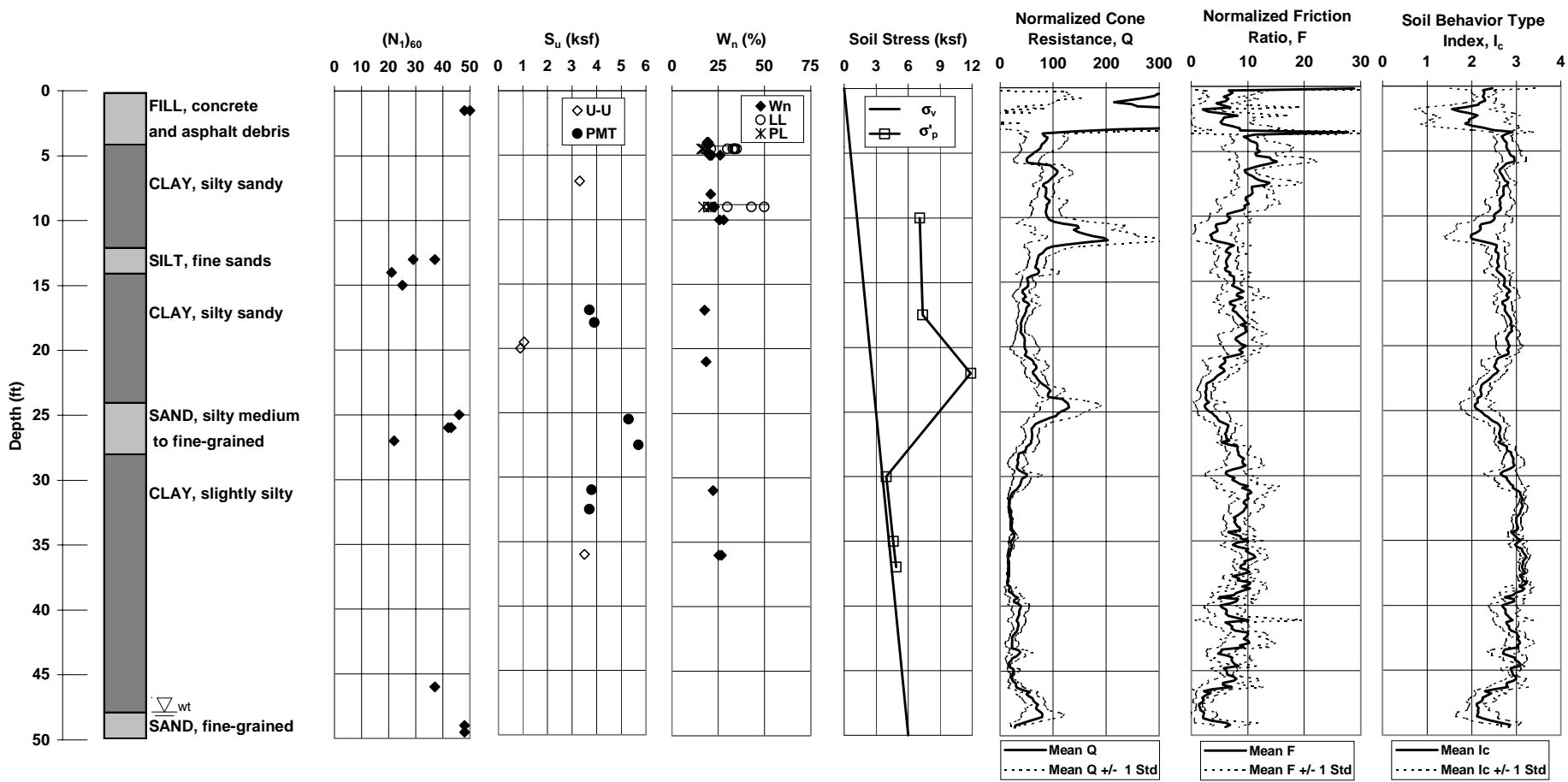


Figure 3: Test site soil profile along with results from field and laboratory investigations

the consolidation tests were approximately 200 ft²/yr (18.6 m²/yr) and 600 ft²/yr (55.8 m²/yr), respectively. Simple consolidation analyses using these data lead us to believe that shearing of the clay during cyclic loading occurred under undrained conditions. Accordingly, triaxial testing of the clay specimens was performed under unconsolidated-undrained conditions, using the procedures described in ASTM D-2850. Specimens were hand-carved from the Pitcher tube samples to an approximate size of 1.3 inch (33 mm) diameter by 3 inch (76 mm) tall. The test results indicated the clay to generally have low sensitivity (< 2) and small failure strains (\approx 0.6 % to 1 %; values of ϵ_{50} were approximately 0.003 to 0.005). Peak strengths from the tests are presented in Figure 3, along with strengths inferred from correlations with limit pressures from in situ pressuremeter testing (Briaud, 1992). Note that the strengths inferred from pressuremeter testing are considerably higher than the laboratory test results. This may reflect a bias in the laboratory test results associated with the fact that only specimens with relatively high clay content could be prepared for triaxial testing, as relatively sandy specimens (of potentially higher strength) de-aggregate during sample trimming. Another reason for the difference could be relatively high matric suction in the in situ soil, which is unsaturated (S=86% to nearly 100% in the tested clay specimens, with an average of 91%).

Test Results and Data Interpretation

Test Results

The relationship between lateral-load and top-of-column lateral peak displacement is shown in Figure 4 for both the first and second cycle at each displacement amplitude. Despite minor soil gapping, the shaft-soil system response was nearly bi-linear up to the yield displacement of approximately 12 inches (305 mm). Yielding of the reinforcement occurred between the 12 and 24 inch (305 and 610 mm) displacement cycles; however, a significant reduction of load capacity was not observed until shaft displacements reached approximately 108 inches (2.7 m). Loss of capacity occurred due to fracture of the longitudinal reinforcement bars approximately 5 ft (1.5 m) below ground line (\approx 0.8d).

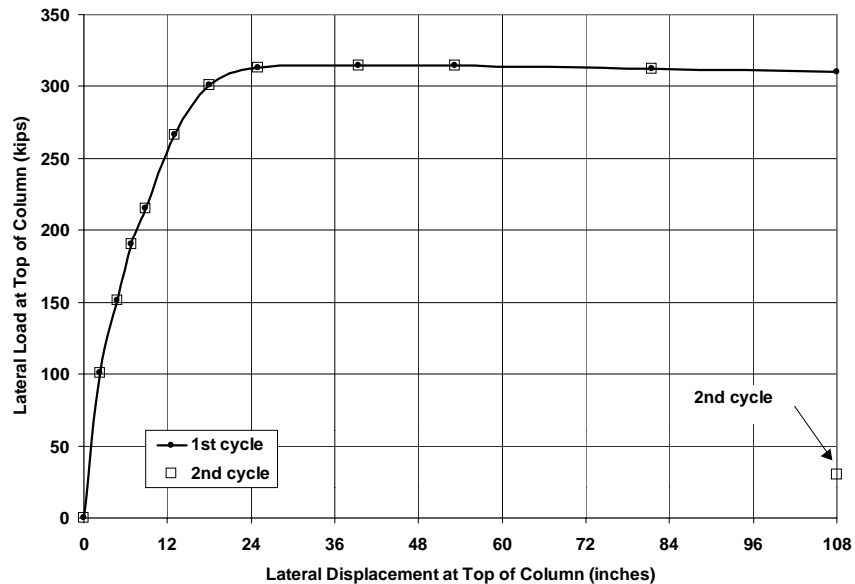


Figure 4: Lateral force-displacement response of test shaft/column

Data Interpretation

In this section, we describe the evaluation of p - y curves from experimental data. Two types of measurements are used for these analyses – slope along the shaft s (measured from inclinometers) and curvature ϕ (measured from extensometer pairs on opposite ends of the shaft section, or inferred based on differentiation of slope with depth). Bending moment is proportional to ϕ , with the constant of proportionality being the nonlinear stiffness of the concrete section, EI ,

$$EI\phi(z) = M(z) \quad (1)$$

where z denotes depth. The lateral soil reaction on the shaft, p , is calculated by double differentiating the shaft bending moment distribution (Hetenyi, 1946),

$$p(z) = \frac{d^2}{dz^2} M(z) \quad (2)$$

The shaft deflected shape, y , is obtained by a single integration of the slope, or a double integration of the curvature. Expressed in terms of differentials, we have,

$$\begin{aligned} \phi(z) &= \frac{d^2}{dz^2} y(z) \\ s(z) &= \frac{d}{dz} y(z) \end{aligned} \quad (3, 4)$$

A complete solution of the differential equations yields a set of profiles such as shown in Figure 5. Several features of the profiles in Figure 5 are noteworthy. First, the y and p profiles cross-over zero at identical depths. Second, boundary conditions used to develop the solution typically include y , s , M , and V at depth zero, and y at the shaft toe (typically assumed to be zero).

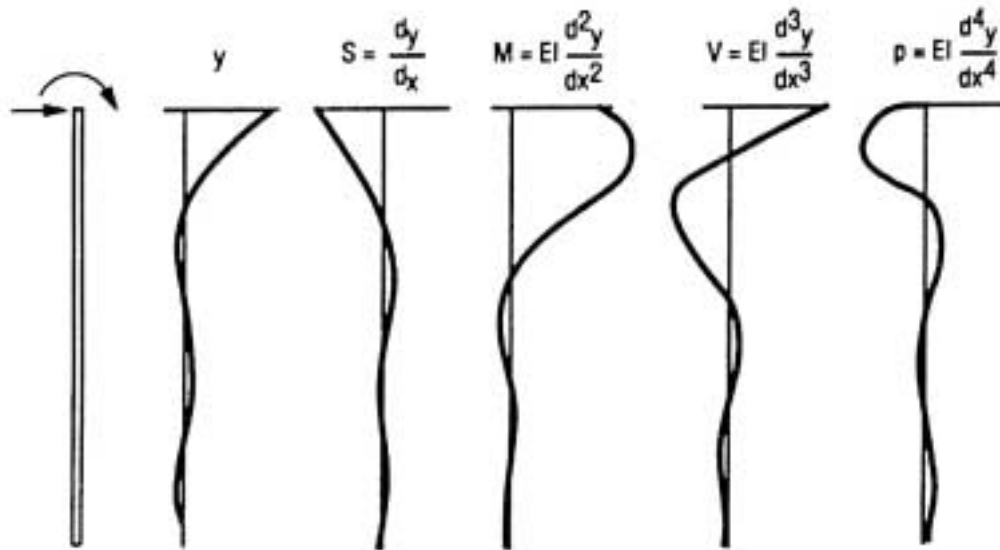


Figure 5: Form of results obtained from a complete solution of a laterally loaded shaft

As noted previously, the flexural stiffness of a reinforced concrete section (EI) is nonlinear, being dependent on ϕ . The relationship between M and ϕ (the secant modulus of which is EI) was evaluated from analysis of the reinforced concrete test section (using the program BIAX, Wallace, 1992) and from direct measurement of ϕ at ground line, which could be related to known M . The moment-curvature analysis of the section utilized results of material testing for both the reinforcing steel and concrete. The effects of concrete confinement were evaluated using a model by Mander (1988). A comparison of the analytical and field-inferred ground line M - ϕ relationship is presented in Figure 6, which shows consistent results. The field-inferred relationship was used in the analyses that follow.

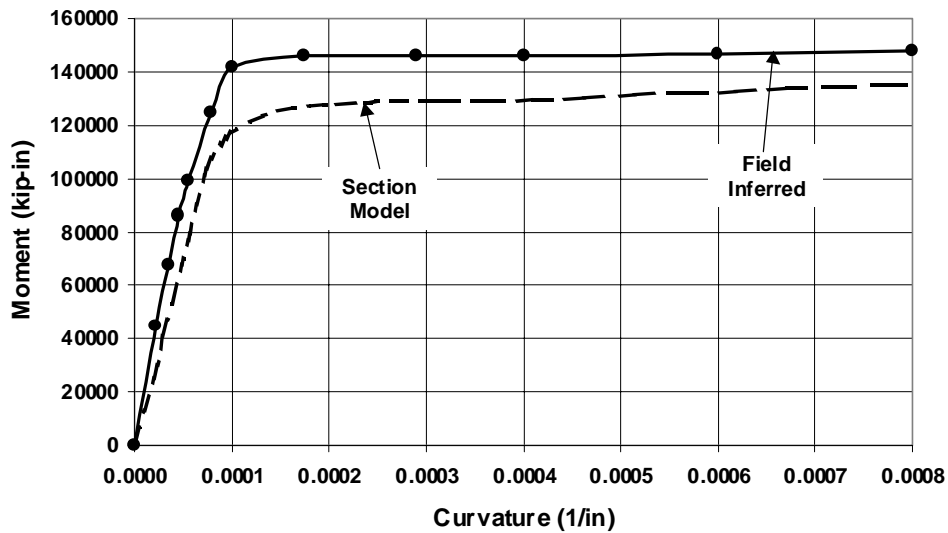


Figure 6: Moment-curvature diagram of test shaft/column from section analysis and experimental data

The shaft deflected shape was evaluated by integrating inclinometer slope data from the ground line down, using the measured ground-line deflection as a boundary condition. This often led to non-zero toe deflection, which is unrealistic for the subject shaft. Accordingly, the slopes were scaled to produce zero toe deflection (scaling factors were typically between 0.72 and 0.78). The left side of Figure 7 shows the scaled slope profile, and the right side shows the calculated deflected shape for the 6 inch (152 mm) displacement level. The above procedure for calculating the shaft deflected shape, y , is relatively stable, i.e., double integration of curvature ϕ provides deflection profiles similar to the single integration of slope s .

Soil reaction, p , was evaluated from redundant curvature measurements using Eq. 1-2 and the M - ϕ relationship in Figure 6. As noted previously, redundant curvature profiles were obtained from the two sets of extensometers, a set of fiber optic sensors, and single differentiation of the slope profile. Figure 8 shows an example of the shaft section curvature distribution from these instruments for the 6 inch (152 mm) displacement level. It is noteworthy that independent sensors produce curvature data with small scatter.

A number of methods for fitting smooth curves through moment profile “data” (inferred from curvature using Eq. 1) were examined, including cubic spline and polynomial fitting functions. An attractive feature of these methods is that they allow p -profiles to be determined through

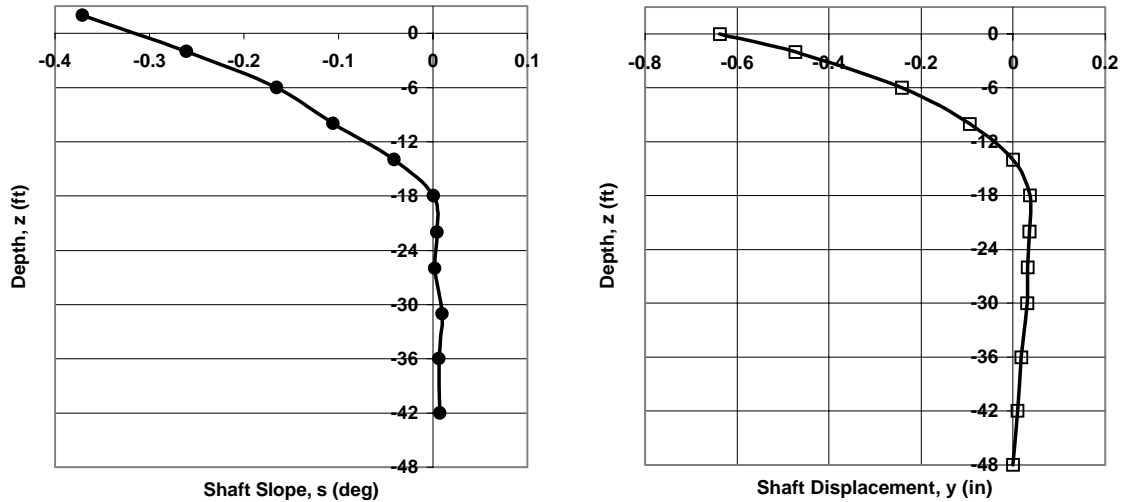


Figure 7: Test shaft slope and deflected shape distributions (6 inch displacement level)

simple, and computationally stable, differentiation of the $M(z)$ function. Unfortunately, such functions could not provide satisfactory fits to the $M(z)$ data at many displacement levels. Accordingly, an alternative data fitting technique known as the weighted residuals method was invoked (Wilson, 1998), which provided more satisfactory results.

As shown in Figure 8, at depths ranging from ground line to -30 ft, there are redundant values of $\phi(z)$ at a given depth z . This measurement of variability in $\phi(z)$ is significant, as small changes in $\phi(z)$ for a given depth produce large variations in $p(z)$ through the double differentiation process.

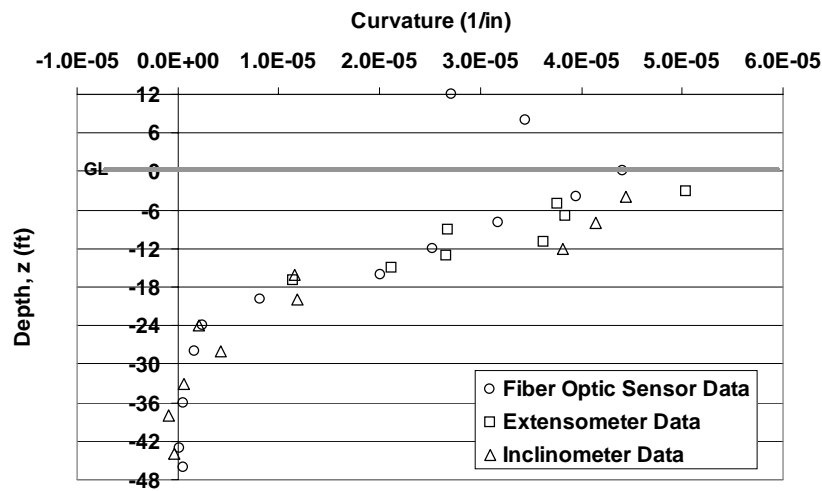


Figure 8: Test shaft curvature distribution using fiber optic sensor, extensometer and inclinometer data (6 inch displacement level)

Each measured value of $\phi(z)$ shown in Fig. 8 is a possible realization of the actual curvature at that depth. Accordingly, we cannot *a priori* eliminate any of these data points, or combinations of data points, as possible realizations of the actual $\phi(z)$. Therefore, multiple profiles of $\phi(z)$ were compiled using each possible value of curvature at depths with multiple measurements. This process led to > 500,000 possible curvature profiles from which $p(z)$ could be evaluated using the weighted residuals approach.

Some $\phi(z)$ profiles obtained by the above approach provide unrealistic results, namely ground line shears that do not match the known value, and $p(z)$ cross-over depths that do not match their $y(z)$ counterpart. Accordingly, constraints were added such that $\phi(z)$ combinations yielding unreasonable ground line shears and $p(z)$ cross-over depths were not considered. Results were considered unreasonable if the ground line shear forces deviate by > 10% from the experimental value, or if zero crossover depths in the $p(z)$ profile deviate from the $y(z)$ crossover by > $d/2$ (3 ft = 0.9 m).

Figure 9 shows the mean, and mean \pm one standard deviation, distributions of $p(z)$ as a function of depth for the case of all possible combinations of measured curvature (left side) and the case when both the ground-line shear and the soil reaction (p) cross-over point were constrained (right side). For most displacement levels, only ~20,000 combinations of curvature measurements satisfied both constraints, which is about 3% of all possible combinations.

The distributions of $p(z)$ shown Figure 9 are derived using the nonlinear flexural stiffness of the reinforced concrete section as described earlier and shown in Figure 6. If the nonlinearity of the section is not considered and a constant effective section stiffness value is used in the analysis of the measured data, the resulting distributions of $p(z)$ are systematically smaller while the distributions of $y(z)$ do not change. This results in p - y curves that can be significantly softer since the nonlinearity of both the shaft section and the shaft-soil interface are lumped in these curves instead just the shaft-soil interface nonlinearity.

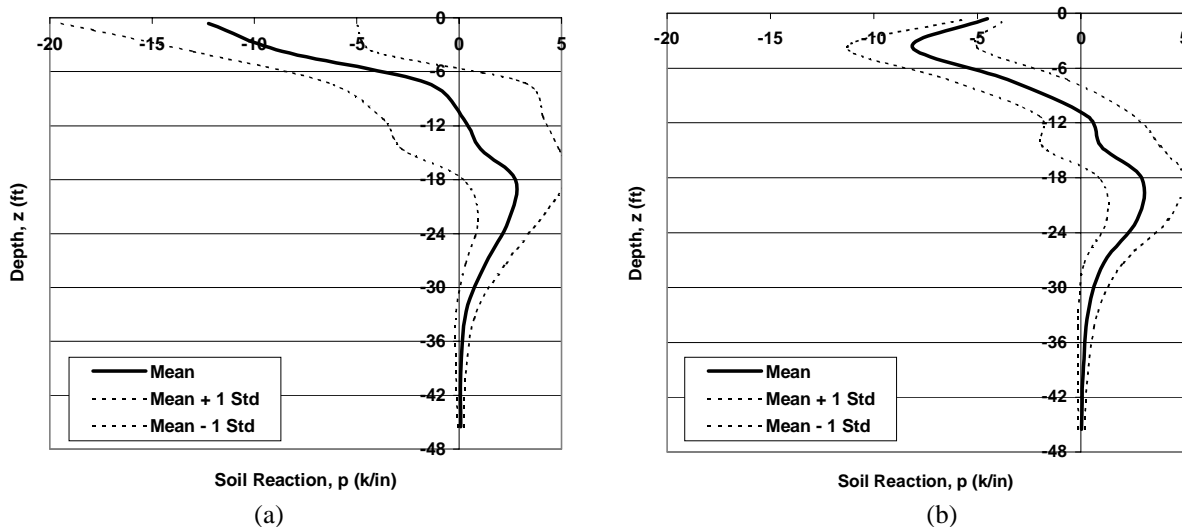


Figure 9: Test shaft soil reaction distribution for (a) all possible combinations of curvature readings, and (b) combinations constrained to ground-line shear values and to soil reaction zero crossover points (6 inch displacement level)

Experimental p - y Curves

The soil reaction, p , and the shaft deflection, y , were calculated along the entire length of the shaft for each of five displacement levels applied during the field test. These data were used to evaluate p - y curves at depths of $d/2$ (3 ft = 0.9 m), $3d$ (18 ft = 5.5 m), $4d$ (24 ft = 7.3 m), and $5d$ (30 ft = 9 m), as shown in Figure 10. The thick lines are the p - y curves at given depths fitted through the mean test data (which are indicated by the solid circles). The calculated mean \pm one standard deviation for each reading of soil reaction p are also shown. Also plotted for comparison are the predicted p - y curves based on in-situ pressuremeter (PMT) test results (Briaud, 1992) and the recommended p - y curves for stiff-clays without free water (Reese and Welch, 1975; API, 1993).

At large depths ($\geq 3d$), the initial modulus of the mean experimental, API, and PMT curves are similar. The mean field-derived curves do not flatten at larger deflections as predicted by the API or PMT curves. The field curves also appear to have higher yield loads. At $z=d/2$, the mean field-derived p - y curves are significantly stiffer than the PMT or API predictions for large displacements. This difference arises because the mean field behavior does not demonstrate the yield at small y (~ 0.005 - 0.2 inches = 0.12 - 5.1 mm) predicted by the API and PMT approaches.

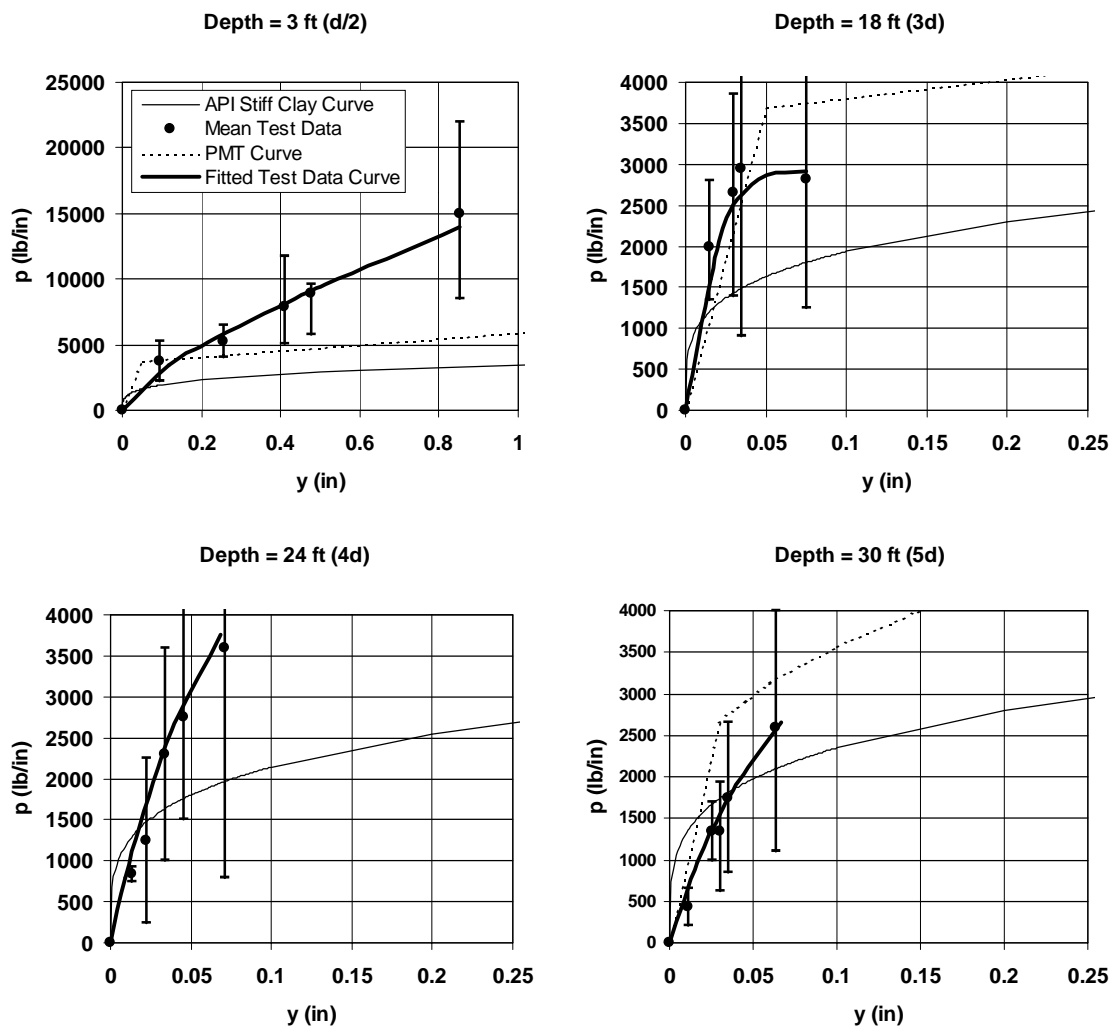


Figure 10: Experimental p - y Curves

Conclusions

So-called p - y curves used in analysis of the lateral response of drilled shaft and pile foundations have typically been developed from field performance data (i.e., lateral load testing). Details associated with the reduction of field data, such as the moment-curvature model and the curve fitting method used to infer the moment profile, can significantly affect the p ordinate in p - y curves. Traditional data reduction approaches that assume constant EI are shown to produce p profiles with potentially significant bias. Moreover, when only a single set of instrumentation is used to evaluate curvature profiles, the resulting p - y curves have an unknown level of reliability. A method for rational analysis of redundant data sources is developed, and provides for the subject site p - y curves generally stiffer and stronger than conventional API curves. Comparisons to PMT curves were somewhat more satisfactory, particularly at large depths ($\geq 3d$).

This paper serves as a report of work in progress. Further work will extend the p - y curves to include results for larger displacement cycles, evaluate the effects of cyclic degradation on p - y curves, and investigate the relative contribution of shear and normal stresses at the soil-shaft interface on the p - y curves. Moreover, further testing will examine smaller diameter shafts so that the diameter effect on p - y curves can be investigated.

Acknowledgements

The research described in this report was carried out with funding from Caltrans, Research Contract No. 59A0183, with Mr. Craig Whitten and Mr. Anoosh Shamsabadi as the Contract Monitors and Mr. Raymond Zelinski as the Contract Manager. The financial support of Caltrans is gratefully acknowledged.

The assistance provided by the staff and students of the Civil & Environmental Engineering Department at UCLA, in particular, Mr. Daniel Whang, Mr. Jeffrey Kent, Mr. Mark Murphy, Mr. Trolis Niebla, Mr. Nirun Tungkongphanit, Mr. David Glass, Mr. Nick Andrews and Mr. Matt Moyneur.

The assistance and support provided by George B. Cooke and Jim Agostino of G.B. Cooke, Inc. is also greatly appreciated, as is the work performed by Malcom Drilling, R.R. Leonard, Gregg In-Situ, A&W Drilling, GeoVision, Mr. Larry Tucker, Geokon, Smartec, and Con-Tech Systems.

References

American Petroleum Institute, API [1993]. *Recommended practice for planning, designing and constructing fixed offshore platforms – Working Stress Design*, Report 2A-WSD, Washington, DC.

Briaud, J.-L. [1992] *The Pressuremeter*, A.A. Balkema Publishing.

Bridge Design Specifications [1995]. California Department of Transportation, CA.

Caltrans Seismic Design Criteria [1999]. California Department of Transportation, CA.

Cox, W.R., L.C. Reese, and B.R. Grubbs [1974]. "Field testing of laterally loaded piles in sand," *Proc., Offshore Tech. Conf.*, Houston, TX, 459-472.

- Hetenyi, M. [1946]. *Beams on Elastic Foundation*, The University of Michigan Press, Ann Arbor.
- Mander, J.B., Priestly, M.J.N., and Park, R. [1988]. "Theoretical stress-strain model for confined concrete," *J. of the Structural Engineering Div.*, ASCE Vol. 114, No. 8, 1804-1826.
- Matlock, H. [1970]. Correlations for design of laterally loaded piles in soft clay, *Proc., 2nd Offshore Tech. Conf.*, Houston, TX., Vol. 1, 577-594.
- Reese, L.C. and W.R. Cox [1968]. "Soil behavior from analysis of tests of uninstrumented piles under lateral loading," *Proc., 71st Annual Meeting*, ASTM, San Francisco, CA, 161-176.
- Reese, L.C., Cox, W.R., and Koop, F.D. [1974]. Analysis of laterally loaded piles in sand, *Proc., 6th Offshore Tech. Conf.*, Houston, TX.
- Reese, L.C., Cox, W.R., and Koop, F.D. [1975]. "Field testing and analysis of laterally loaded piles in stiff clay," *Proc., 7th Offshore Tech. Conf.*, Houston, TX, 671-690.
- Reese, L.C. and R.C. Welch [1975]. "Lateral loading of deep foundations in stiff clay," *J. of the Geotechnical Engineering Div.*, ASCE, Vol. 101, No. GT7, 633-649.
- Robertson, P.K. (1990). "Soil classification using CPT," *Canadian Geotechnical J.*, 27 (1), 151-158.
- Wallace, J.W. [1992]. "BIAX; Revision 1: A computer program for the analysis of reinforced concrete and reinforced masonry sections," Report No. CU/CEE-92/4, Structural Engineering, Mechanics and Materials, Clarkson University.
- Wilson, D.W. [1998] "Soil-pile-superstructure interaction in liquefying sand and soft clay." Ph.D. Dissertation, Univ. of California, Davis.